

# Electrochemical characterizations of precipitates formed on zinc in alkaline sulphate solution with increasing pH values

Stephan Bonk, Mariusz Wicinski, Achim Walter Hassel\*, Martin Stratmann

*Max-Planck-Institut für Eisenforschung GmbH, Max-Planck-Strasse 1, 40237 Düsseldorf, Germany*

Received 13 May 2004; accepted 14 May 2004

Available online 17 June 2004

## Abstract

Increased alkalinity during oxygen reduction contributes largely to corrosion and polymer degradation on galvanized steel. In these investigations, studies have been carried out to quantify the pH dependence of the electrochemical properties for pure zinc under alkaline conditions. In contrast to theoretical predictions, a strong kinetic influence is observed for intermediate to high alkaline pH values, resulting in an anodic shift of the corrosion potential and corresponding changes in the electrochemical properties of the surface layer. Also, a significant delay in the potential stabilisation is observed for pH values assigned to the increase, respectively, decrease to this found potential maximum. As an explanation a precipitant layer of various zinc complexes is suggested that changes its structure and composition with variation of the pH. For pH values below 12 it has a more homogeneous and compact structure. In the pH range between 12 and 13 the structure becomes inhomogeneous and porous. For higher pH values than 13 it changes back to the homogenous and compact structure.

© 2004 Elsevier B.V. All rights reserved.

*Keywords:* Zinc; pH-Dependence; Precipitate; EIS; Alkaline solution

## 1. Introduction

Zinc is used in a wide range of applications by various industries, e.g. as a construction material for roofs and facades in structural and civil engineering or as a sacrificial coating to protect iron and steel products from environmental corrosion attack in the steel producing and processing industry, especially the automotive industry [1,2]. The atmospheric corrosion attack of zinc depends on many different parameters such as temperature, contaminations, humidity, etc. This results in very complex corrosion mechanisms that have yet to be understood, especially for those of zinc plated steel. In case of intact protective zinc layers on steel experiments have shown that alkalinisation due to oxygen reduction plays

a key role in the corrosion mechanism and the delamination of polymers [3,4].

The experimental work presented here focuses on the issues of zinc stability and the pH dependence of its electrochemical properties like corrosion potential and interface capacitance. Results from experiments using a pH range between 7 and 14 are presented. These experiments were performed to monitor and understand the fundamental processes and behaviour of pure zinc under those alkaline conditions.

## 2. Experimental

Pure bulk zinc with a purity of 99.5% (ALFA ASEAR) was investigated. Cylindrical samples with a diameter of 10 mm and a thickness of 1 mm were used. Specimen surfaces were ground and polished, followed by ultrasonic cleaning in ethanol. Finally, the samples were rinsed thoroughly with distilled water.

\* Corresponding author. Tel.: +49-211-6792-464; fax: +49-211-6792-218.

*E-mail address:* [hassel@elchem.de](mailto:hassel@elchem.de) (A.W. Hassel).

A typical electrochemical three electrode arrangement was used to measure the electrochemical properties in alkaline media. The reference electrode is a commercial silver/silver chloride electrode (METROHM Ag/AgCl, filled with 3 M KCl), and a gold counter electrode was used. The samples were mounted into a specially designed Teflon sample holder that exposes a well defined surface area ( $\approx 50.27 \text{ mm}^2$ ) while protecting the electrical connectors from contact with the electrolyte. This arrangement was immersed completely into an aerated sodium sulphate solution ( $\text{Na}_2\text{SO}_4$ ). The pH of the solution was changed stepwise in the range between 7 and 14 adding 0.1 M sodium hydroxide solution for pH values below 10, respectively, 1 M sodium hydroxide solution for higher pH values.

For every adjusted pH value the open circuit potential transient has been taken over a time period of 10 min. After stabilisation of the potential, an impedance spectra measurement was carried out. After the impedance spectroscopy, the open circuit potential was measured again for 1 min and compared with the potential values before the impedance measurements. This ensures that no changes caused maybe by the impedance spectroscopy were ignored. Based on both collected data sets a mean potential was calculated for every adjusted pH.

For data acquisition a standard PC connected to a Solartron Potentiostat 1287 and a Frequency Response Analyser 1255B was used.

### 3. Results

Fig. 1 shows the measured corrosion potential transients for some selected pH values. For the pH values of

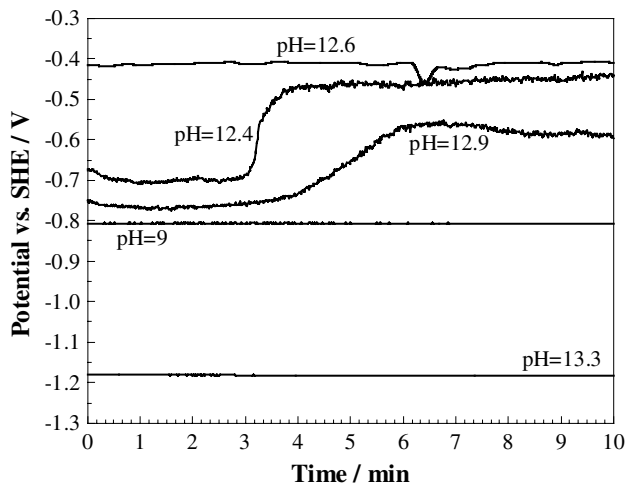


Fig. 1. Measured potential transients on zinc in aerated 0.1 M  $\text{Na}_2\text{SO}_4$  solution for different pH values adjusted with NaOH. The transients for pH = 12.4 and 12.9, assigned to the increase, respectively, decrease to a potential maximum at pH = 12.6 (see Fig. 2), show a significant delay in the potential stabilisation.

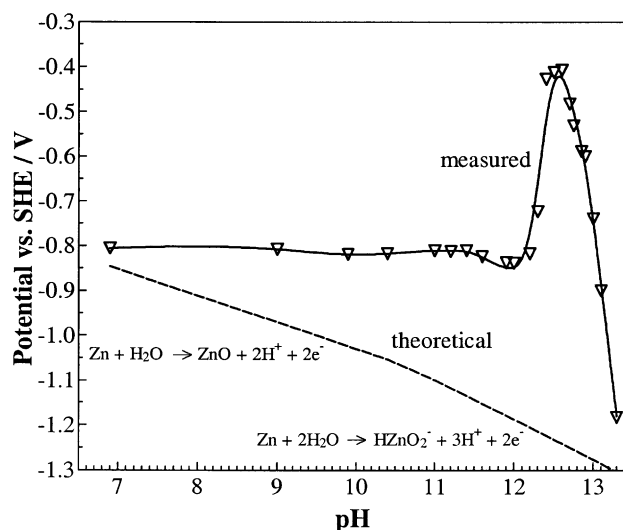
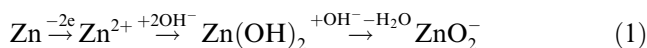


Fig. 2. Corrosion potentials of zinc in aerated 0.1 M  $\text{Na}_2\text{SO}_4$  at different pH values adjusted with NaOH. The potential values were estimated from the potential transients for the particular pH after the potential has been stabilized (see Fig. 1). The theoretical line is calculated based on thermodynamic aspects and hydroxylation at the interface.

12.4 and 12.9 a significant delay of several minutes in the potential stabilisation and a higher fluctuation in the measured potential values was observed. For all other transients, also for those, that are not shown here for the sake of clarity, the potential always attains stability almost immediately. The potential also shows much fewer or no fluctuations during the measurement. With regard to the mean potential values, shown in Fig. 2, these two exceptional pH values were assigned to the increasing, respectively, decreasing side of a potential maximum at pH = 12.6. For higher or lower pH values the estimated potentials are always more electronegative. It can be seen in Fig. 2 that in the lower pH range, between pH = 7 and 11, the averaged potential remains constant at approximately  $-800 \text{ mV SHE}$ . It begins to rise in the range between pH = 12 and 13 to more anodic values with a maximum of  $-400 \text{ mV SHE}$  at pH = 12.6. For pH values above pH = 13 the potential then drops to the theoretically predicted values, given by the dotted line. It represents the theoretical potential behaviour following the electrochemical reaction path regarding hydroxylation at the interface and thermodynamical aspects [5,6]



The plotted averaged potential values in Fig. 2 were estimated for the particular pH after the potential has been stabilized, e.g. after 4 min for pH = 12.4 (see Fig. 1).

The results of the impedance spectroscopy measurements reveal a similar trend. Some selected spectra are shown in Fig. 3. For pH values between pH = 12 and 13 an increase of the impedance amplitude  $|Z|$  for low

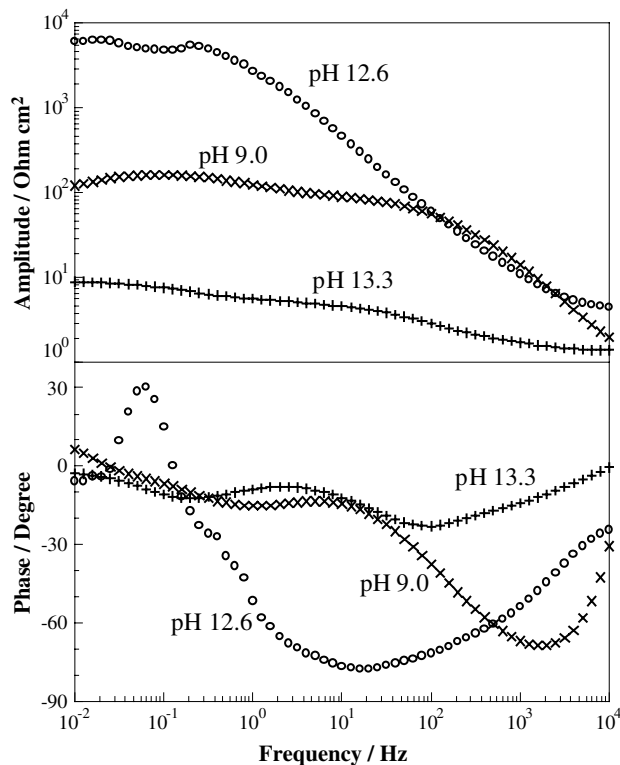


Fig. 3. Measured impedance spectra on zinc in aerated 0.1 M Na<sub>2</sub>SO<sub>4</sub> solution for different pH values adjusted with NaOH. The spectra assigned to the potential maximum at pH = 12.6 shows a significant higher impedance amplitude  $|Z|$  for low frequencies as in case of the other two shown spectra for pH = 9.0 and pH = 13.3. Coupled to this rise is also a greater instability in the measured phase of the taken spectra for the low frequencies.

frequencies ( $\sim 10^{-2} \dots 10^{-1}$  Hz) were observed, followed by a sudden decrease after the maximum at pH = 12.6. Coupled to this rise is also a greater instability in the measured phase of the taken spectra for the low frequencies. In order to analyse the impedance data, a model based on a precipitate layer with both the possibilities of electron and ion transfer through the layer has been used [7,8]. The equivalent circuit is shown in Fig. 4. The transfer function of this circuit is given by

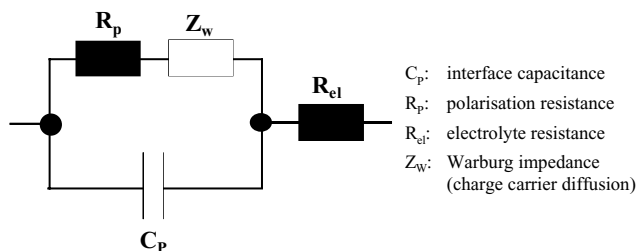


Fig. 4. Equivalent circuit used for fitting the data from the impedance measurements. It is based on the model of a precipitate layer on top of the zinc surface allowing electron and ion transfer as the charge carrier transport mechanism.

$$Z(f) = R_{el} + \frac{R_p + Z_w(f)}{1 + \{R_p + Z_w(f)\}i2\pi f C_p}. \quad (2)$$

Here,  $f$  means the frequency,  $C_p$  the interface capacitance,  $R_p$  the polarisation resistance, and  $R_{el}$  the electrolyte resistance. The Warburg impedance  $Z_w$  is given by the equation

$$Z_w(f) = R_D \frac{\tanh\{\sqrt{i2\pi f T}\}}{\sqrt{i2\pi f T}}, \quad (3)$$

where  $R_D$  is the diffusion resistance and  $T$  is the relaxation time constant. The used expression for the Warburg impedance is the short circuit behaviour form which takes into account the discharge of the ion charge carriers by contact with the metallic surface [9,10].

Normally, this complex transfer function (2) is an 8-dimensional fitting problem. Every of the four electrical components in the equivalent circuit (see Fig. 4) is described by a value in the 2-dimensional complex plane. Due to the fact that the resistors  $R_{el}$  and  $R_p$  are given by real values and the capacitance  $C_p$  has only a complex contribution to the transfer function the fitting problem is reduced to 5 dimensions. Nevertheless, the complex non-linear least square fit of this function delivers a large number of mathematical existing, but physical and chemical non relevant solutions for the equation system, e.g. with negative values for the resistors. To avoid running into such pure mathematical results in the fitting process, the electrochemical parameters of the transfer function are estimated in a first approximation from the behaviour for low and high frequencies. For low frequencies Eq. (2) becomes

$$\lim_{f \rightarrow 0} Z(f) = R_{el} + R_p + R_D, \quad (4)$$

a serial combination of the electrolyte resistance, the polarisation resistance and the diffusion resistance of the layer. In case of high frequencies the transfer function (2) tends to be a linear combination of the electrolyte resistance and the interface capacitance,

$$\lim_{f \rightarrow \infty} Z(f) = \underbrace{R_{el}}_{\text{Re}\{Z(f)\}} + i \underbrace{\frac{-1}{2\pi f C_p}}_{\text{Im}\{Z(f)\}}. \quad (5)$$

By using the approximations (4) and (5) the interface capacitance  $C_p$  is calculated from the imaginary part of the impedance data for high frequencies and the sum  $R_p + R_D$  of the diffusion and polarisation resistance is estimated from the real part of the low frequency impedance data. The results are shown in Fig. 5. The interface capacitance is more or less stable over the whole pH range whereas the sum of the polarisation and diffusion resistance is increasing in the area of the potential maximum. It was also observed, that the electrolyte resistance  $R_{el}$ , which is given by the real part of the high frequency data, is nearly constant over the whole pH

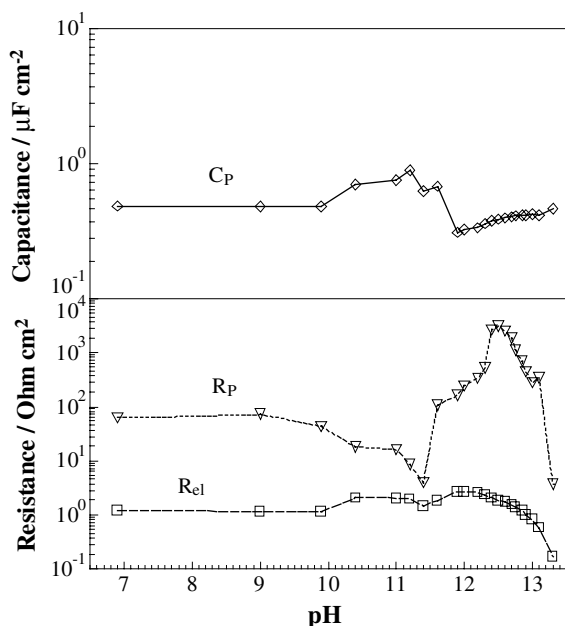


Fig. 5. Values for the interface capacitance and the polarisation resistance of the surface and the forming layer gained from performed impedance spectroscopic measurements on zinc in aerated 0.1 M  $\text{Na}_2\text{SO}_4$  at different pH values adjusted with NaOH.

range until high pH values are reached. For pH-values above 12 the concentration of the  $\text{OH}^-$ -ions becomes greater than those of the  $\text{SO}_4^{2-}$ -ions therefore dominating the conductivity of the electrolyte. Regarding this and the effect of extraordinary conductivity of water and its ions, a decrease of the electrolyte resistance  $R_{el}$  was caused.

#### 4. Discussion

The results can be explained by assuming the formation of a thin and inhomogeneous layer of precipitates on the surface of the sample. For near neutral  $\text{Na}_2\text{SO}_4$  solutions a complex surface morphology of the corroded zinc surface was found by Sziráki et al. [8]. By XRD, SEM, and TEM techniques they observed on top of a compact layer consisting of Zn and ZnO porous deposits which contain embedded sulphur in the form of zinc-hydroxy-sulphate  $\text{Zn}_4\text{SO}_4(\text{OH})_6$ . They also found that the structure of these deposits depend on the concentration of the  $\text{Na}_2\text{SO}_4$  solution, the higher the concentration the more porous the precipitate layer is. Following these results it is supposed that in the case of near neutral pH values a nearly compact layer of precipitates, mainly Zn and ZnO, with small amounts of  $\text{Zn}(\text{OH})_2$ , is present on the surface. During the adjustment of the different pH values, anions are diffusing into this layer and reacting with the zinc cations to form various zinc complexes. This results in a change of the

structure, the composition and the thickness of the layer, making it more porous. Due to these changes also the type of charge carrier transport is changing from electron to ion transfer. This can be observed in the rise of the overall layer resistance shown in Fig. 5 and the potential increase in Fig. 1. These compositional and structural changes are responsible also for the delay in the potential stabilisation in case of the pH values assigned to the increase, respectively, decrease to the potential maximum (see Fig. 2).

It is believed that the composition of the layer in these potential maximum area is mainly  $\text{Zn}(\text{OH})_2$  and  $\text{Zn}_4\text{SO}_4(\text{OH})_6$ , which would correspond with the fact that the pH range between 10 and 13 is the predominance area of the bizincate ion  $\text{HZnO}_2^-$  [6], a first important stage in the formation of the above mentioned zinc molecules. Above pH 13 the bizincate ion becomes less dominant and is replaced by the zincate ion  $\text{ZnO}_2^{2-}$  as the dominant ion. This causes again a change in the composition and structure of the layer back to the more compact form consisting of the Zn and ZnO species. A direct result is the sudden drop in the potential and the resistance (see Figs. 1 and 5) as the charge carrier transport mechanism is changing back from ionic to electron transfer.

#### 5. Conclusions

The simplified model used to predict theoretically the electrochemical behaviour of pure zinc in alkaline media does not take into account the strong kinetic influence of the compositional and structural changes in the precipitate layer. The carried out measurements show that due to ongoing reactions in the precipitate layer, assigned to the formation and destruction of various zinc complexes, a strong deviation from the theoretical values can be observed in the pH range between 12 and 13. By extending the model to a precipitate layer which is changing its structure from homogeneous and compact to an inhomogeneous and porous state most of the observed effects can be explained.

For an exact identification of the different formed zinc complexes and their formation or dissolution in-depth experiments has to be carried out dealing with direct in situ spectroscopic measurements of the layer's composition during the different adjusted pH values. This should give an insight into the reaction mechanism for developing an advanced model of the behaviour of zinc in alkaline media with changing pH.

Also the question of applicability of these results to zinc coated steel will be a main point of further investigations. Experiments with different types of protective zinc coatings on steel are carried out at the moment to specify the influence of different elements, e.g. Al, added to the zinc coating material.

## Acknowledgements

The authors are thankful for the financial support by the European Coal and Steel Community (ECSC), Contract.- No. 7210-PR/256. We are indebted to our project partners K. Ogle of IRSID-Usinor, K.-H. Stellnberger of Voest-Alpine Stahl, Linz; and C. Ostwald of DOC/TKS, Dortmund – for useful discussions.

## References

- [1] F.M. Androsch, K. Kösters, K.-H. Stellnberger, *Stahl Eisen* 121 (2001) 37.
- [2] A.R. Marder, *Prog. Mater. Sci.* 45 (2000) 191.
- [3] W. Fürbeth, M. Stratmann, *Fres. Anal. Chem.* 353 (1995) 337.
- [4] W. Fürbeth, M. Stratmann, *Prog. Org. Coat.* 39 (2000) 23.
- [5] N. Sato, in: N. Sato (Ed.), *Electrochemistry at Metal and Semiconductor Electrodes*, Elsevier Science, Amsterdam, 1998 (Chapter 5.11.1).
- [6] N. de Zoubov, M. Pourbaix, in: M. Pourbaix (Ed.), *Atlas of Electrochemical Equilibria*, National Association of Corrosion Engineers, 1974 (Chapter 15.1).
- [7] J. Hazan, J. Yahalom, *Corros. Sci.* 35 (1993) 223.
- [8] L. Sziráki, Á. Cziráki, I. Geröcs, Z. Vértesy, L. Kiss, *Electrochim. Acta* 43 (1998) 175.
- [9] I.D. Raistrick, in: J.R. Ross Macdonald (Ed.), *Impedance Spectroscopy*, Wiley, New York, 1987 (Chapter 2.1.3).
- [10] J.R. Macdonald, D.R. Franceschetti, in: J.R. Macdonald (Ed.), *Impedance Spectroscopy*, Wiley, New York, 1987 (Chapter 2.2.2.2).